



Effect of atmospheric anisoplanatism on earth-to-satellite time transfer over laser communication links

ANICETO BELMONTE,^{1,*} MICHAEL T. TAYLOR,² LEO HOLLBERG,³ AND JOSEPH M. KAHN²

¹Technical University of Catalonia, Department of Signal Theory and Communications, 08034 Barcelona, Spain

²Stanford University, E. L. Ginzton Laboratory, Department of Electrical Engineering, Stanford, CA 94305, USA

³Stanford University, Hansen Experimental Physics Laboratory, Department of Physics, Stanford, CA 94305, USA

*belmonte@tsc.upc.edu

Abstract: The need for an accurate time reference on orbiting platforms motivates study of time transfer via free-space optical communication links. The impact of atmospheric turbulence on earth-to-satellite optical time transfer has not been fully characterized, however. We analyze limits to two-way laser time transfer accuracy posed by anisoplanatic non-reciprocity between uplink and downlink. We show that despite limited reciprocity, two-way time transfer can still achieve sub-picosecond accuracy in realistic propagation scenarios over a single satellite visibility period.

© 2017 Optical Society of America

OCIS codes: (060.2605) Free-space optical communication; (010.1300) Atmospheric propagation; (120.3940) Metrology.

References and links

1. A. Bauch, "Time and frequency comparisons using radiofrequency signals from satellites," *C. R. Phys.* **16**(5), 471–479 (2015).
2. F. Riehle, "Optical clock networks," *Nat. Photonics* **11**(1), 25–31 (2017).
3. K. Djerroud, O. Acef, A. Clairon, P. Lemonde, C. N. Man, E. Samain, and P. Wolf, "Coherent Optical Link through the Turbulent Atmosphere," *Opt. Lett.* **35**(9), 1479–1481 (2010).
4. E. Samain, P. Vrancken, P. Guillemot, P. Fridelance, and P. Exertier, "Time Transfer by Laser Link (T2L2): Characterization and Calibration of the Flight Instrument," *Metrologia* **51**(5), 503–515 (2014).
5. F. R. Giorgetta, W. C. Swann, L. C. Sinclair, E. Baumann, I. Coddington, and N. R. Newbury, "Optical two-way time and frequency transfer over free space," *Nat. Photonics* **7**(6), 434–438 (2013).
6. L. C. Sinclair, F. R. Giorgetta, W. C. Swann, E. Baumann, I. Coddington, and N. R. Newbury, "Optical phase noise from atmospheric fluctuations and its impact on optical time-frequency transfer," *Phys. Rev. A* **89**(2), 023805 (2014).
7. J.-D. Deschênes, L. C. Sinclair, F. R. Giorgetta, W. C. Swann, E. Baumann, H. Bergeron, M. Cermak, I. Coddington, and N. R. Newbury, "Synchronization of Distant Optical Clocks at the Femtosecond Level," *Phys. Rev. X* **6**(2), 021016 (2016).
8. P. Berceau, M. Taylor, J. M. Kahn, and L. Hollberg, "Space-time reference with an optical link," *Class. Quantum Gravity* **33**(13), 135007 (2016).
9. P. Fridelance, "Influence of atmospheric turbulence on the uplink propagation in an optical time transfer," *Appl. Opt.* **36**(24), 5969–5975 (1997).
10. C. Robert, J. Conan, and P. Wolf, "Impact of turbulence on high-precision ground-satellite frequency transfer with two-way coherent optical links," *Phys. Rev. A* **93**(3), 033860 (2016).
11. D. Kirchner, "Two-way time transfer via communication satellites," *Proc. IEEE* **79**(7), 983–990 (1991).
12. V. I. Tatarski, *Wave Propagation in a Turbulent Medium* (McGraw-Hill, 1961).
13. L. C. Andrews and R. L. Phillips, *Laser Beam Propagation Through Random Media* (SPIE, 2005).
14. R. J. Sasiela, *Electromagnetic wave propagation in turbulence: evaluation and application of Mellin transforms* (Springer-Verlag, 1994).
15. R. J. Sasiela and J. D. Shelton, "Transverse spectral filtering and Mellin transform techniques applied to the effect of outer scale on tilt and tilt anisoplanatism," *J. Opt. Soc. Am. A* **10**(4), 646–660 (1993).
16. R. R. Parenti and R. J. Sasiela, "Laser-guide-star systems for astronomical applications," *J. Opt. Soc. Am. A* **11**(1), 288 (1994).

17. J. H. Shapiro, "Reciprocity of the turbulent atmosphere," *J. Opt. Soc. Am.* **61**(4), 492–495 (1971).
18. R. F. Lutomirski and H. T. Yura, "Propagation of a finite optical beam in an inhomogeneous medium," *Appl. Opt.* **10**(7), 1652–1658 (1971).
19. R. J. Hill and S. F. Clifford, "Modified spectrum of atmospheric temperature fluctuations and its application to optical propagation," *J. Opt. Soc. Am.* **68**(7), 892–899 (1978).
20. G. Ling and R. Gagliardi, "Slot Synchronization in Optical PPM communications," *IEEE Trans. Commun.* **34**(12), 1202–1208 (1986).
21. R. Paschotta, "Noise of mode-locked lasers (Part II): timing jitter and other fluctuations," *Appl. Phys. B* **79**(2), 163–173 (2004).
22. R. M. Gagliardi and S. Karp, *Optical Communications* (Wiley & Sons, 1995).
23. A. Belmonte and J. Khan, "Performance of synchronous optical receivers using atmospheric compensation techniques," *Opt. Express* **16**(18), 14151–14162 (2008).
24. D. L. Fried, "Optical heterodyne detection of an atmospherically distorted signal wave front," *Proc. IEEE* **55**(1), 57–77 (1967).
25. D. L. Fried, "Anisoplanatism in adaptive optics," *J. Opt. Soc. Am.* **72**(1), 52–61 (1982).
26. J. W. Goodman, *Speckle Phenomena in Optics. Theory and Applications* (Ben Roberts & Company, 2007).
27. J. Goodman, *Introduction to Fourier Optics*, (Roberts & Company, 2005).
28. J. G. Proakis and M. Salehi, *Digital Communications*, (Mc Graw-Hill, 2007).
29. E. Ip and J. M. Kahn, "Power spectra of return-to-zero optical signals," *J. Lightwave Technol.* **24**(3), 1610–1618 (2006).

1. Introduction

Timing and synchronization are indispensable components of many modern technologies. Precise, accurate timing is essential in many ground-based systems, including communication networks, data centers, smart power grids, and financial exchanges. Likewise, precise timing is required in many space-based systems supporting technology and fundamental science, including satellite communications, global satellite navigation, very-long-baseline interferometry observation, and deep space exploration. The transfer of precise clock signals between Earth and space can benefit all these ground- and space-based systems.

Highly precise and reliable time synchronization between Earth and space is a complex undertaking that must account for time-dilation relativistic effects, rotating-frame Sagnac effects, Earth-geoid gravitational anomalies, and the influence of other objects in the solar system. Despite the challenges, time transfer between atomic clocks on Earth and in space via microwave signals is widely used and can reach nanosecond levels of accuracy [1].

Time transfer between Earth and space via free-space optical links may offer distinct advantages over microwave systems for future timing needs requiring extreme precision and accuracy [2]. The potential advantages of free-space optical methods for such time and frequency transfer have long been recognized. For example, coherent optical links have been considered for satellite Doppler ranging and long-distance frequency transfer [3]. A laser link experiment has been designed for synchronization of remote ultra-stable clocks over intercontinental distances using satellite laser ranging technology with dedicated equipment for recording laser pulse arrival times at the satellite [4]. Recent experiments on the ground have demonstrated picosecond-level synchronization of distant optical clocks by measuring arrival times of pulses from optical frequency combs [5,6]. Remarkably, in a recent two-way experiment on the ground, femtosecond-level synchronization of distant optical clocks has been achieved by measuring arrival times of pulses from femtosecond optical frequency combs [7], suggesting the possibility of achieving such performance on Earth-to-space optical links.

Exploiting free-space laser communication links between Earth and space for time transfer is particularly attractive [8]. These links already provide pointing and tracking means, and already require accurate timing for efficient signal decoding. Free-space optical communication requires accurate temporal synchronization of a receiver to periodic pulse edges or waveform zero crossings to achieve low-error-rate signal decoding. Since performance degrades rather quickly as timing error increases, receiver decoding clocks must be accurate within a fraction of the symbol interval, typically at the sub-nanosecond level.

Refractive index fluctuations caused by atmospheric turbulence are known to degrade the spatial and temporal coherence of received data-bearing optical signals. Turbulence is likewise expected to limit the accuracy of time transfer over free-space links [9], as the clock signal phase and arrival time become random variables that fluctuate about some mean values. The impact of atmospheric turbulence on earth-to-space optical time transfer has not been fully characterized. In this paper, we identify the turbulence mechanisms that fundamentally limit time and frequency accuracy in two-way time transfer over free-space optical communication links, and we analytically quantify the limits they pose. A recent work [10] addressed two-way time transfer over coherent free-space optical links, studying the impact of turbulence through detailed end-to-end simulations. This work addressed the potential benefits of atmospheric compensation in two-way links between Earth and space, finding that tip-tilt control to correct the downlink and pre-compensate the uplink mitigates atmospheric effects, improving time transfer precision. The simulation-based study [10] complement the analysis presented here and its results are mainly consistent with ours.

The remainder of this paper is organized as follows. In Section 2, we describe the turbulence mechanisms that affect two-way optical time transfer with an orbiting platform. Depending on whether an optical clock signal is conveyed directly via a carrier phase or is instead borne via a modulation signal imposed on the carrier, the transferred clock phase is affected by fluctuations in the atmospheric phase index or group index, respectively. For concreteness, we consider the impact of group index fluctuations on modulated clock-bearing signals. Atmospheric index variations are nearly achromatic, so turbulence is expected to have a nearly identical impact on clock signals conveyed via the carrier phase. In Section 3, we define a mathematical model describing propagation of a clock signal through the atmosphere. We provide analytical expressions for the time transfer variances due to atmospheric fluctuations and detection noises. These variances are expressed in terms of parameters describing the atmospheric turbulence conditions, the signal strength, and the photodetection methods employed. In Section 4, we use those analytical expressions to study the effect of various parameters on time transfer standard deviation. We present discussion and conclusions in Section 5.

2. Two-way optical time transfer in orbit

Both intensity and phase fluctuations induced by atmospheric turbulence impact free-space time transfer. Intensity fluctuations lead to random fluctuations in received signal strength. Phase fluctuations cause complex distortions of the received signal wavefront. Higher-order phase distortions are typically filtered out by the receiver optical system (often by a low-numerical aperture optical fiber), but impact coupling efficiency, causing additional fluctuations in received signal strength similar to those produced by intensity fluctuations. Fluctuation of the lowest-order piston component corresponding to the delay of the propagation path ultimately poses the major limitation for one-way free-space time transfer. In a one-way time transfer system, a terminal at one end of the link transmits its current time to a receiver at the other end. A major drawback of one-way time transfer is that propagation delay fluctuations of the atmospheric channel are entirely uncompensated.

We consider two-way time transfer [11] to obtain partial cancellation of atmospheric effects. In this method, signals are sent in two directions, enabling comparison between clock phase measurements made by terminals on the ground (at time T_G) and at a satellite (at time T_S), as shown in Fig. 1. Each terminal includes a time interval counter that is initialized to

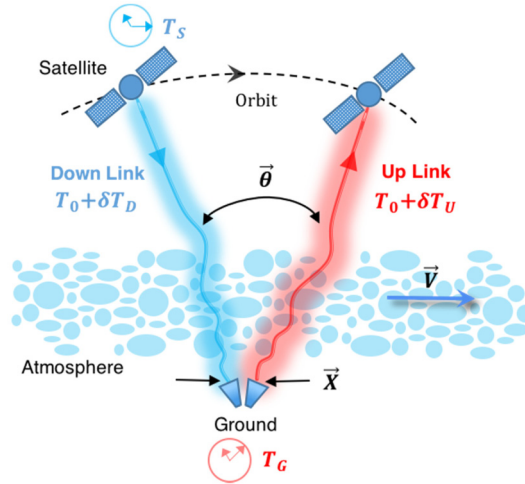


Fig. 1. Schematic of two-way time transfer over a satellite laser communication link for providing a high-accuracy time reference. Time transfer may benefit from the low clock jitter in such laser communication links, but will be degraded by atmospheric fluctuations leading to time-of-flight variations. Incomplete reciprocity between the uplink and downlink propagation paths translates into temporal, spatial, and angular atmospheric anisoplanatic effects that limit the accuracy of two-way time transfer. As described in the text, this analysis considers anisoplanatic effects over a medium-earth-orbit (MEO) altitude of 9000 km.

zero when it transmits a counter value to the other terminal. Upon receiving a counter value from the other terminal, a terminal stops its counter, subtracts the counter value received from the other terminal from its own counter value, and sends its counter value to the other terminal. Through this process, the measurements $\Delta T_G = (T_S + T_0 + \delta T_D) - T_G$ and $\Delta T_S = (T_G + T_0 + \delta T_U) - T_S$ are made by the terminals on the ground and the satellite, respectively.

Here, T_0 describes the nominal optical propagation delay between the ground and the satellite, and δT_U and δT_D are residual delays on the uplink and downlink paths, correspondingly. The time difference between the clocks $\tau = T_G - T_S$ is

$$\tau = \frac{1}{2} [(\Delta T_S - \Delta T_G) - (\delta T_U - \delta T_D)]. \quad (1)$$

The accuracy of two-way time transfer clearly depends on the accuracy of characterizing the residual delays δT_U and δT_D . Typically, the residual delays can be broken into deterministic and random components. The deterministic components are a function of the particular optical and electronic equipment used in the measurements, and can be calibrated before comparing the clocks. By contrast, the random components, including those caused by atmospheric turbulence and by noise in the optical detection process, cannot be eliminated through calibration. The measurement accuracy of the time transfer τ is ultimately limited by the random components, which lead to a time transfer variance σ_τ^2 . Usually, time measurements are carried out in measurement periods of variable duration—ranging from a few seconds to several hundred seconds—during which pulse-to-pulse measurements are made at the two receiving terminals.

In any earth-to-satellite link, spatio-temporal displacement between the uplink and downlink propagation paths leads to anisoplanatic non-reciprocity. This causes the time-of-flight fluctuations for the two paths to differ, imposing limits on the accuracy of two-way

time transfer. We analyze those limits here, also considering the impact of noise encountered in signal detection. The spatio-temporal displacement between propagation paths considered here is shown in Fig. 1. Asymmetry is induced by the point-ahead angle $\bar{\theta}$ because of the finite velocity of light and the relative angular velocity of the orbiting terminal. During the time t_d required for signals to propagate between the terminals, the turbulence is displaced at relative velocity \bar{V} by wind and by slewing of the satellite. In some cases, the ground-based transmitter and receiver apertures are displaced from one another by a distance \bar{X} . These various path asymmetries define a vector displacement between the two paths $\bar{d}(z) = \bar{X} + \bar{\theta}z + \bar{V}(z)t_d$. We have assumed that the uplink and downlink beams are collimated, and have used the fact that the point-ahead angle is very small in ground-satellite links. The general geometry shown in Fig. 1 can describe most important types of anisoplanatism, including angular anisoplanatism $\bar{\theta}z$, temporal anisoplanatism $\bar{V}(z)t_d$, and anisoplanatism induced by aperture separation \bar{X} .

3. Effect of anisoplanatism on time transfer

The random temporal delay of a pulse propagating through a random medium is caused primarily by two mechanisms: wandering of the beam and dispersive scattering caused by propagation via multiple paths. Beam wandering is the dominant factor causing random delay in propagation through the turbulent atmosphere. Pulses arrive at the receiver with variable path delays as they travel over spatially different paths. Propagation through turbulence causes a loss of spatial coherence, which causes fluctuations in power coupling in the receiver. Our analysis includes intensity fading caused by this effect, although its impact on time transfer is negligible. This effect can be much stronger, and potentially non-negligible, when scattering by turbid constituents of the atmosphere occurs.

The time-of-flight variation through an atmospheric path of length L caused by index fluctuations is given by $\delta T_{atm} = (1/c) \int_0^L dz \delta n(z,t)$, where the optical beam propagates along the z direction, c is the speed of light in vacuum, and $\delta n(z,t)$ is the atmospheric refractive index variation. The classical theory of atmospheric turbulence provides an analytical characterization of $\delta n(z,t)$ that can be used to express the atmospheric time-of-flight variance as [12,13]

$$\sigma_{\delta T_{atm}}^2 = \frac{2\pi}{c^2} \int_0^L dz \int d\bar{K} \Phi_n(\bar{K}, z). \quad (2)$$

In (2), $\Phi_n(\bar{K}, z)$ is the power spectral density of the refractive fluctuations $\delta n(z,t)$ at two-dimensional spatial frequency \bar{K} . Expressions for $\Phi_n(\bar{K}, z)$ are provided below. The ergodic variance in (2), defined as an ensemble average over many independent realizations of the atmosphere, is a meaningful measure of time transfer uncertainty because the time scale for channel variations (typically ms) is short compared to the time scale for time transfer measurements (typically s).

In two-way propagation along a horizontal path between ground-based terminals, a high degree of path reciprocity may lead to small vector displacement $\bar{d}(z)$ and effective minimization of time-of-flight variance [6]. By contrast, in earth-to-satellite links, large spatial and temporal displacements between uplink and downlink paths cause significant anisoplanatic non-reciprocity, potentially causing errors in two-way time transfer. To analyze

how these errors depend on the displacement $\vec{d}(z)$ between the uplink and downlink paths, we employ the method of transverse spectral filtering on turbulence [14]. A similar approach has been used to quantify anisoplanatism-induced errors in laser guide star adaptive optics systems [15,16]. It should be mentioned that the impact of turbulence on a beam propagating downward to the ground can be modeled accurately by considering propagation of a plane wave. Furthermore, the well-known principle of reciprocity in propagation through turbulence indicates that the impact of turbulence on uplink propagation can also be inferred from study of the downward-propagating plane wave [17,18]. Consequently, there is no need to consider upward propagation, nor any impact of the laser beam spatial distribution.

In the transverse spatial filtering method, one considers an amplitude filter function $h(\vec{K}, z)$ [14], which describes how turbulence fluctuations common to the two propagation paths are removed during two-way time transfer. This allows us to express the time-of-flight variance in two-way time transfer $\sigma_{\tau_{\text{atm}}}^2$ as

$$\sigma_{\tau_{\text{atm}}}^2 = \frac{2\pi}{c^2} \int_0^L dz \int d\vec{K} \Phi_n(\vec{K}, z) |h(\vec{K}, z)|^2. \quad (3)$$

Given a path displacement $\vec{d}(z)$, the amplitude filter function for two-way time transfer is given by

$$h(\vec{K}, z) = 1 - \exp[j \vec{K} \cdot \vec{d}(z)]. \quad (4)$$

The filter $h(\vec{K}, z)$ described by Eq. (4) has a simple physical interpretation: any displacement \vec{d} between the two propagation paths in the spatial domain corresponds to a complex phase factor $\exp[j \vec{K} \cdot \vec{d}(z)]$ in the spatial frequency domain. As one expects intuitively, in two-way transfer over a highly reciprocal link, the displacement is small, $\vec{d} \rightarrow 0$, which leads to $h(\vec{K}, z) \rightarrow 0$ and negligible time-of-flight variance, $\sigma_{\tau_{\text{atm}}}^2 \rightarrow 0$.

Substituting Eq. (4) into Eq. (3) and expressing the dot product as $\vec{K} \cdot \vec{d}(z) = Kd(z)\cos(\psi)$, where ψ is the angle between the vectors \vec{K} and \vec{d} , Bessel's first integral can be applied to simplify Eq. (3) as

$$\sigma_{\tau_{\text{atm}}}^2 = \frac{4\pi^2}{c^2} \int_0^L dz \int K dK \Phi_n(K, z) 2\{1 - J_0[K d(z)]\}, \quad (5)$$

where J_0 denotes the Bessel function of the first kind of order 0. We will model the turbulence spectrum as $\Phi_n(K, z) = 0.033 C_n^2(z) f(K) K^{-11/3}$ [13], where the refractive-index structure parameter $C_n^2(z)$ describes the turbulence strength, which can vary along the propagation path, and $f(K)$ parameterizes turbulence scales. When $f(K) = 1$, the Kolmogorov spectrum is obtained. That spectrum is often assumed because it facilitates theoretical calculations. Assuming $f(K) = 1$ allows us to integrate Eq. (5) over K to obtain a simple 5/3-power dependence of the time-of-flight variance on path displacement d , i.e., $\sigma_{\tau_{\text{atm}}}^2 = (2.914/c^2) \int_0^L dz C_n^2(z) d^{5/3}(z)$. This result is of limited utility, however, because it includes the effects of unphysical turbulence scales. Hence, we assume the more realistic Von

Kármán spectrum [13] $f(K) = \left[1 + (K_o/K)^2\right]^{-11/6} \exp\left[-(K/K_i)^2\right]$, where $K_o = 1/L_o$ and $K_i = 5.92/l_o$ depend on the outer scale parameter L_o and the inner scale parameter l_o , respectively. Hill's modified spectrum [19] and Greenwood-Tarazano's empirical spectrum [6] also extend the Kolmogorov spectrum to consider both outer and inner scales of turbulence.

Using Taylor's frozen turbulence assumption, in which the only change in turbulence is due to wind transport, one obtains an equivalence between time delays and spatial shifts. Taylor's hypothesis is a central assumption invoked in most experiments designed to investigate turbulence effects via temporal integration measurements. If t is the characteristic time scale of the problem, the spatial frequency K is related to the temporal frequency $f = 1/t$ by $K = 2\pi f/V$, where $V = V(z)$ is the relative velocity induced by wind and by slewing of the satellite. In our analysis, the time-of-flight variance averaged over a measurement interval of $1/B_c$ s, where B_c is the measurement bandwidth, can be written as

$$\sigma_{\tau_{am}}^2 = \frac{4\pi^2}{c^2} \int_0^L dz \left(\frac{2\pi}{V}\right)^2 \int f df \Phi_n\left(\frac{2\pi f}{V}, z\right) 2 \left\{1 - J_0\left[\frac{2\pi f}{V} d(z)\right]\right\}, \quad (6)$$

where the integral with respect to f extends over the range $B_c < f < V/l_o$. The power spectrum $\Phi_n(2\pi f/V, z)$ flattens at frequencies f below V/L_o .

Time transfer over free-space communication links benefits from the low clock jitter that must be achieved in such links. Noise in the photodetection process (e.g., shot noise and thermal noise) limits the clock timing accuracy to the scale of tens of femtoseconds. We assume that for the sake of efficiency, the transferred clock signal is embedded in a data stream, and the receiver synchronizes its local clock to the sequence of received data pulses. We consider how noise in photodetection causes fluctuations in the measured pulse arrival times, and thus the local clock. The mean fluctuation is zero, and the variance of the pulse arrival time can be expressed in terms of the reciprocal of the received signal-to-noise ratio (SNR) over a measurement interval [20,21]. Assuming the data pulses have a Gaussian shape with full width at half-maximum (FWHM) duration T_p , the variance of the pulse position averaged over a measurement interval of $1/B_c$ s can be written as

$$\sigma_{\tau_{clk}}^2 = 0.1803 B_c \frac{T_p^2}{\Omega \gamma_0}, \quad (7)$$

where γ_0 is the SNR per unit time. The factor Ω represents a mean receiver coupling efficiency describing fading caused by atmospheric turbulence, so $\gamma = \Omega \gamma_0$ describes the average SNR per unit time in the presence of turbulence. In practice, a link must be designed such that the SNR γ is sufficient to achieve a required bit-error ratio (BER). Note that if $\Omega \gamma_0$ is held constant, the variance given by Eq. (7) is larger for longer pulse duration T_p .

If a receiver employs ideal local oscillator shot noise-limited coherent detection, the SNR per unit time γ_0 equals the received number of signal photons per second, K_s . If a receiver instead employs direct detection, possibly using an optical preamplifier or avalanche photodetector with noise figure F , and is subject to a thermal noise K_n and background noise K_b , the SNR per unit time becomes [22]

$$\gamma_0 = \frac{K_s^2}{F(K_s + 2K_b) + K_n}. \quad (8)$$

A simple PIN photodiode receiver is described by choosing $F=1$ and $K_s=0$ in the denominator. An avalanche photodiode receiver is described by choosing a noise figure $F = \alpha_p G + (2 - 1/G)(1 - \alpha_p)$, where G is the avalanche gain and α_p is the ratio of hole to electron avalanche ionization coefficients. An optically preamplified receiver, where the optical gain helps to make receiver thermal noise K_n negligible, is described by choosing a noise figure F equal to twice the amplifier spontaneous emission coefficient n_{sp} .

In the presence of atmospheric turbulence, amplitude and phase fluctuations cause random fading in the signal coupled to the receiver described by the mean coupling efficiency Ω in Eq. (7). Amplitude and phase fluctuations, and the corresponding value of Ω , need to be characterized [23]. Here, we assume the log-amplitude χ and phase ϕ fluctuations are Gaussian-distributed, characterizing them by their respective variances $\sigma_\chi^2 = (1/4) \ln(1 + \sigma_\beta^2)$ and $\sigma_\phi^2 = 1.0299(D/r_0)^{5/3}$. The intensity variance σ_β^2 is often referred to as the scintillation index [13]. The aperture diameter D of the optical receiving system is normalized to the wavefront coherence diameter r_0 , which describes the spatial correlation of phase fluctuations in the aperture plane [24,25]. In this model, the power fading Ω can be described by a non-central chi-square random variable with two degrees of freedom. The model leading to this distribution is based in the observation that a received signal can be characterized as the sum of many contributions from different coherence regions within the aperture [26,27]. The power fading Ω depends inversely on the number of coherence areas within the aperture $N \approx (D/r_0)^2$ and can be expressed as the sum of a constant (coherent) term and a random (incoherent) residual halo [23]:

$$\Omega = \alpha_0^2 + 2\sigma_\alpha^2, \quad (9)$$

where $\alpha_0^2 = \exp(-\sigma_\chi^2) \exp(-\sigma_\phi^2)$ is the strength of the coherent component and $2\sigma_\alpha^2 = (1 - \alpha_0^2)/N$ is the strength of the residual halo. The ratio $r = \alpha_0^2 / 2\sigma_\alpha^2$ is a measure of the strength of the coherent component relative to the halo.

4. Time transfer uncertainty analysis

In this section, we evaluate the time transfer uncertainty in a representative ground-satellite link, considering the impact of anisoplanatic non-reciprocity and noise encountered in detection.

The Von Kármán atmosphere model considered here exhibits turbulence on length scales between 10 mm and 100 m, which corresponds to the inner and outer turbulence scales l_o and L_o , respectively. We have considered several other values for the outer scale L_o , ranging from several m to several hundred m, but with minimal effects on our estimates of time transfer uncertainty. Beyond the convenient Von Kármán model, we have also considered other turbulence spectra, such as Hill's modified spectrum and Greenwood-Tarazano's empirical spectrum. In general, as long as the turbulence models exhibit a spectrally flat behavior at spatial frequencies below $1/L_o$, time transfer uncertainty is minimally affected by the specific shape of the power spectrum.

We model the profile of turbulence structure constant C_n^2 on the downlink using the Hufnagel-Valley (H-V) model [13]. The model depends on the structure constant at the ground C_{n0}^2 , and the rms wind speed $V(z)$ along the optical path. We assume $V(z)$ is described by the Buffon pseudo-wind model using the ground wind speed and the slew rate

associated with satellite motion relative to an observer on the ground. Without loss of generality, and as a relevant practical example, we assume an elevation angle $\varphi = 45^\circ$ and a moderate-to-strong ground structure constant $C_{n0}^2 = 10^{-14} m^{-2/3}$. The profile of C_n^2 determines the scintillation index σ_β^2 and the phase coherence diameter r_0 . Assuming a wavelength $\lambda = 1550$ nm, the scintillation index is $\sigma_\beta^2 \approx 0.6$, and the coherence diameter is $r_0 \approx 10$ cm. We assume a receiver aperture diameter $D = 40$ cm. The power fading parameter, which depends inversely on the number of coherence areas within the aperture, $(D/r_0)^2$, has a value $\Omega \approx -12$ dB.

We estimate the time transfer uncertainty over different measurement intervals up to a maximum representing a typical satellite-ground station visibility window. Considering a medium-earth-orbit altitude of 9000 km, the orbital period is about 5 hours and the visibility window is over one hour. In the assumed orbit, the elevation angle changes at a slew rate of about 0.3 mrad/s. For the assumed orbital parameters, uplink and downlink signals are time-displaced by about $t_d = 30$ ms, and the required point-ahead-angle is about $\theta = 35$ μ rad. We assume the ground-based transmit and receive apertures are separate but immediately adjacent, so that $X = D$.

We evaluate the performance of time transfer over laser communication links assuming binary differential phase-shift keying at a bit rate of 1 Gb/s. We assume the received power is sufficient to achieve $\text{BER} = 10^{-6}$, so the number of signal photons per second is $\gamma \approx 25 \times 10^9$ [28]. For the 1550-nm wavelength and 40-cm aperture considered in this analysis, this level of signal photons corresponds to an acceptable satellite downlink power density at the ground of about 35 nW/m², assuming a 75% quantum efficiency. The power budget includes a 12-dB margin to guard against coupling losses and fading, which is sufficient for most practical atmospheric conditions. We consider 33% duty-ratio return-to-zero pulses and model them by Gaussian pulses with FWHM duration equal to one third of a bit period [29], i.e., $T_p = 1/3$ ns.

Figure 2 presents the total time transfer standard deviation $\sigma_\tau = (\sigma_{\tau_{\text{atm}}}^2 + \sigma_{\tau_{\text{clk}}}^2)^{1/2}$ as a function of measurement time $1/B_c$, where the variances from atmospheric turbulence and detection noise, $\sigma_{\tau_{\text{atm}}}^2$ and $\sigma_{\tau_{\text{clk}}}^2$, are given by Eqs. (6) and (7), respectively. The result for a shot noise-limited coherent receiver is shown as a solid blue line. For this coherent receiver, the results with total reciprocity ($h(\vec{K}, z) \rightarrow 0$ so that $\sigma_{\tau_{\text{atm}}}^2 \rightarrow 0$) and with no reciprocity ($\sigma_{\tau_{\text{atm}}}^2$ computed assuming $h(\vec{K}, z) \rightarrow 1$) are shown for reference as dashed blue lines. The time-of-flight standard deviation induced by turbulence $\sigma_{\tau_{\text{atm}}}$ is also shown for comparison as a dashed blue line. As seen in the plots, for short measurement intervals of order one second, the detection noise contribution $\sigma_{\tau_{\text{clk}}}$ is the main source of uncertainty, and the turbulence contribution $\sigma_{\tau_{\text{atm}}}$ can be neglected. Although the detection noise contribution $\sigma_{\tau_{\text{clk}}}$ decreases linearly with the integrated number of photons detected, the turbulence contribution $\sigma_{\tau_{\text{atm}}}$ becomes important only at measurement times of several s or longer. A measurement interval of several tens of s, well below the expected satellite visibility window, yields a total time transfer standard deviation σ_τ under 10 fs. Measurement times above a few seconds do not

further improve time transfer precision, which approaches the limit imposed by atmospheric turbulence, $\sigma_\tau \approx \sigma_{\tau_{atm}}$, a limit of several fs.

Figure 2 also shows the total time transfer standard deviation $\sigma_\tau = (\sigma_{\tau_{atm}}^2 + \sigma_{\tau_{clk}}^2)^{1/2}$ considering suboptimal detection methods, where $\sigma_{\tau_{clk}}^2$ is computed using SNR per unit time γ_0 given by Eq. (8). Using a simple PIN photodiode receiver (solid black line) with its high thermal noise level ($K_n \approx 1$), the atmospheric turbulence limit can be approached only for unrealistically long measurement times. An avalanche photodiode receiver (solid green line) with parameters $K_n \approx 390$, $K_b \approx 2$, $\alpha_p = 0.2$, and $G = 105$ provides higher precision, but still approaches the atmospheric turbulence limit only for measurement times of several hundred s. An optically preamplified receiver (solid red line) with $n_{sp} = 1.4$ approaches the performance of a shot noise-limited coherent receiver and the atmospheric turbulence limit for measurement times of about 10 s.

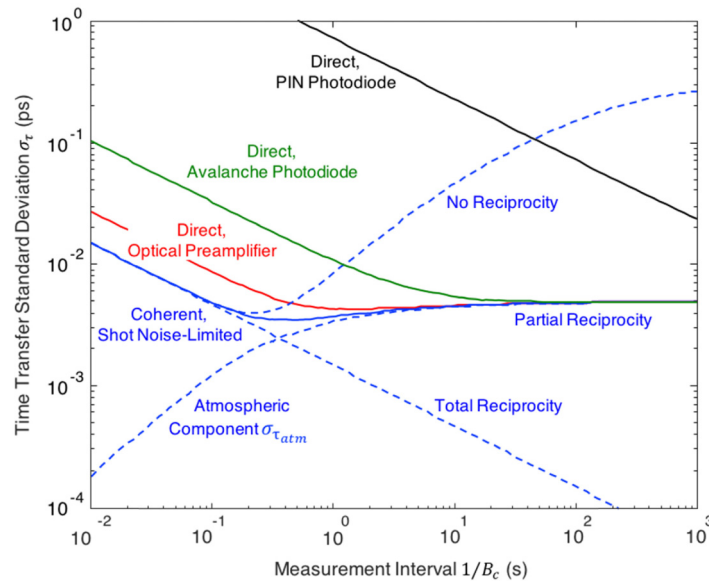


Fig. 2. Analytically predicted time transfer standard deviation σ_τ as a function of measurement interval $1/B_c$ considering partial reciprocity between up and down propagation paths. Receivers considered employ: shot noise-limited coherent detection (blue), direct detection with optical pre-amplifier (red), direct detection with avalanche photodiode (green) and direct detection with PIN photodiode (black). For the coherent receiver, the curves with total reciprocity (identical up and down propagation paths) and without reciprocity (independent up and down propagation paths) are shown as dashed blue lines for comparison. The corresponding component of the time-of-flight standard deviation induced by turbulence $\sigma_{\tau_{atm}}$ is also shown.

5. Discussion and conclusions

Our analysis suggests that, despite fundamental atmospheric anisoplanatic effects, earth-to-satellite laser communication links can support time transfer with fs precision. We note that the saturation of time transfer precision at longer measurement intervals that we predict (Fig. 2) was not seen in the simulation-based study [10], which considered shorter measurement times and significantly different inner and outer scale lengths, and employed tip-tilt control to

correct the downlink and pre-compensate the uplink. The apparent differences between our findings and those in [10] can be resolved through further analysis and experiments. In preliminary ongoing work, we find that incorporating tip-tilt correction mitigates non-reciprocity, and saturation of time transfer precision is seen only at measurement intervals above 10 s, well beyond the measurement times considered in [10]. We expect that atmospheric compensation can also mitigate the impact of turbulence on power coupling to the receiver, which may be particularly helpful for short measurement intervals.

Our results demonstrate that using an optical communication link for time transfer is a promising method for precise synchronization of space-based clocks and time/frequency transfer between ground and space. We have shown that despite limited reciprocity between uplink and downlink propagation, partial two-way cancellation of atmospheric effects occurs, making precision time transfer possible over a single satellite visibility period in realistic propagation scenarios. Our analytic model shows that a direct-detection two-way laser communication link can provide sub-picosecond timing between ground and space. This approach could support the next generation of atomic clocks, geodetic references, and global navigation satellite systems [8].

Funding

NASA Fundamental Physics Program.

Acknowledgments

The authors are grateful to P. Wolf and N. Newbury for helpful discussions about their efforts and free-space optical time/frequency transfer in general.